Electronic Supporting Information (ESI)

Mesoporous Carbon Cubes Derived from Fullerene Crystals as a High Rate Performance Electrode Material for Supercapacitors

Partha Bairi,[a] Subrata Maji,[a] Jonathan P. Hill,[a] Jung Ho Kim,[b] Katsuhiko Ariga [a,c] and Lok Kumar Shrestha[a]*

[a]*International Center for Materials Nanoarchitectonics (WPI-MANA), National Institute for Materials Science (NIMS), 1-1 Namiki, Tsukuba 305-0044, Japan*
[b]*Institute for Superconducting and Electronic Materials (ISEM), Australian Institute for Innovative Materials (AIIM), University of Wollongong, North Wollongong, NSW 2500, Australia*
[c]*Graduate School of Frontier Science, The University of Tokyo, Kashiwa, Chiba 277-0827, Japan*

Contact: SHRESTHA.Lokkumar@nims.go.jp

Contents

1. SEM images of MCFC

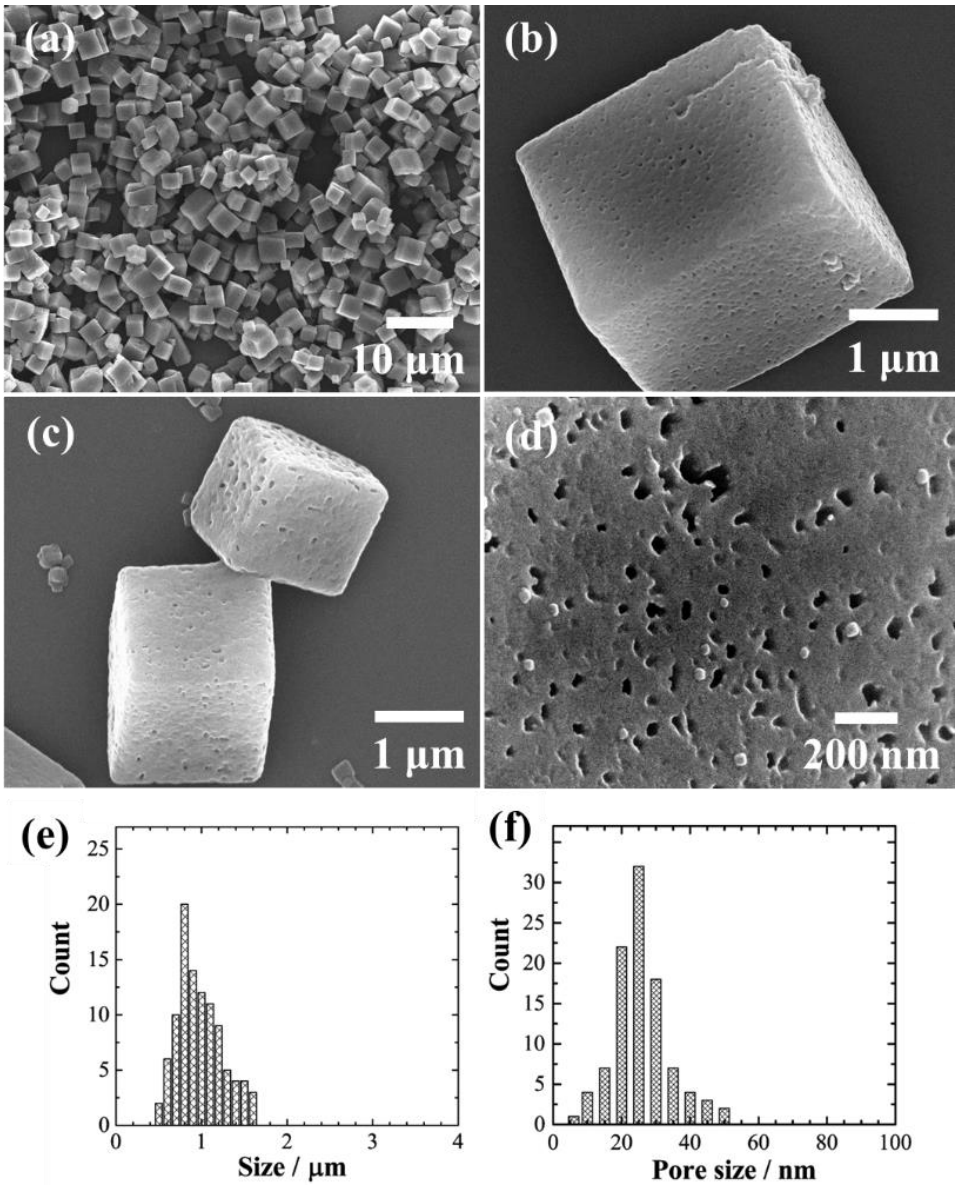

Figure S1: (a-d) SEM images of MCFC. (e) Edge size distribution of MCFC. (f) Pore size distribution of MCFC.

2. TEM observations of MCFC

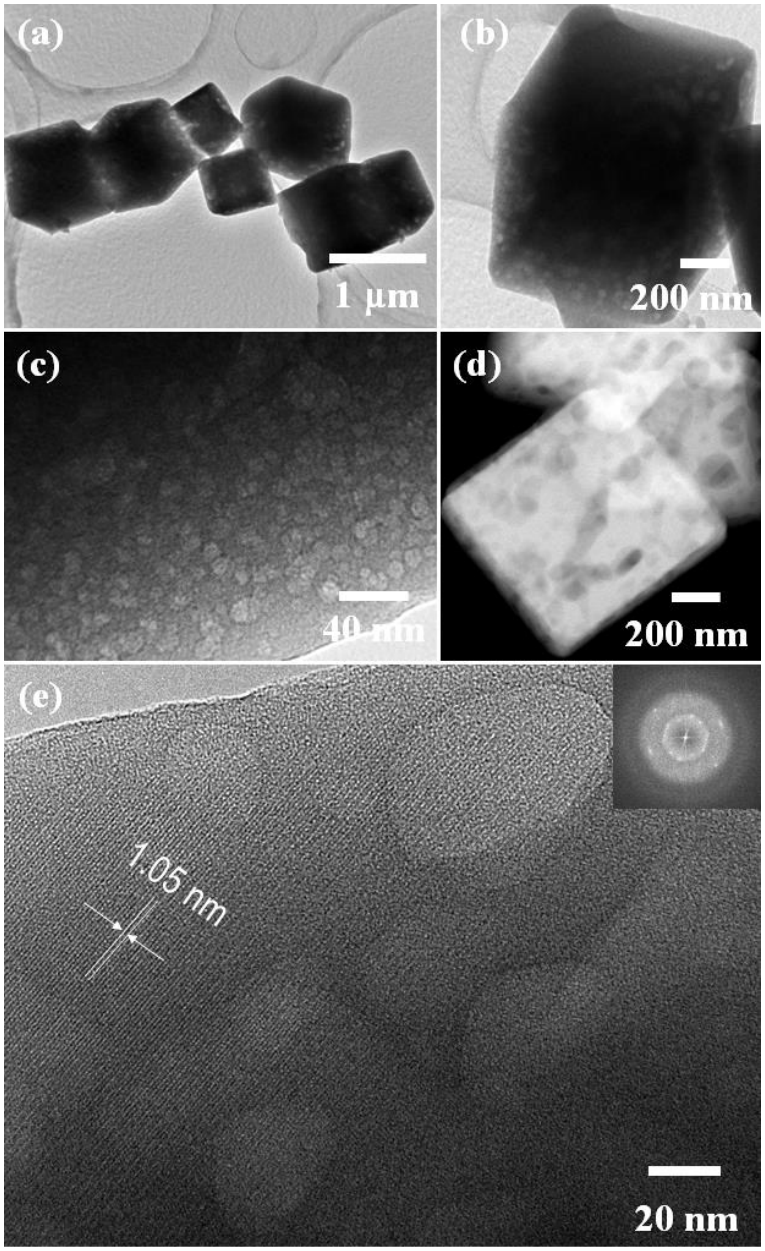

Figure S2: (a-c) and (d) TEM and STEM images of MCFC, respectively. (e) HR-TEM image of the MCFC.

3. FT-IR spectra and Thermogravimetric Analysis of MCFC

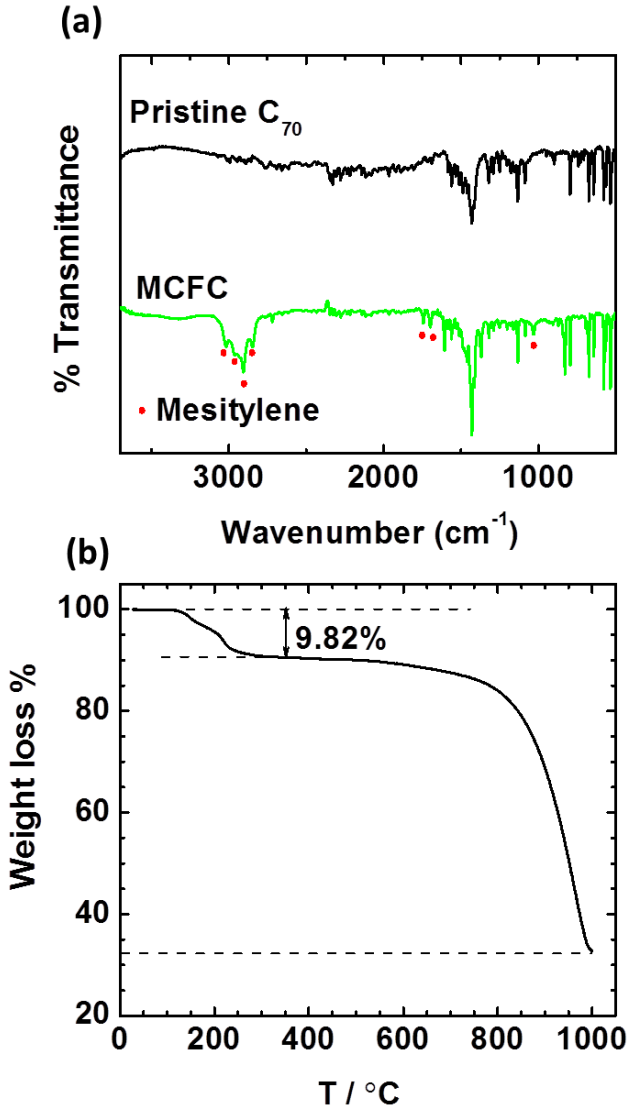

Figure S3: (a) FT-IR spectra of MCFC and together with pristine C_{70} and (b) thermogravimetric analysis of MCFC.

4. SEM images of MCFC-900

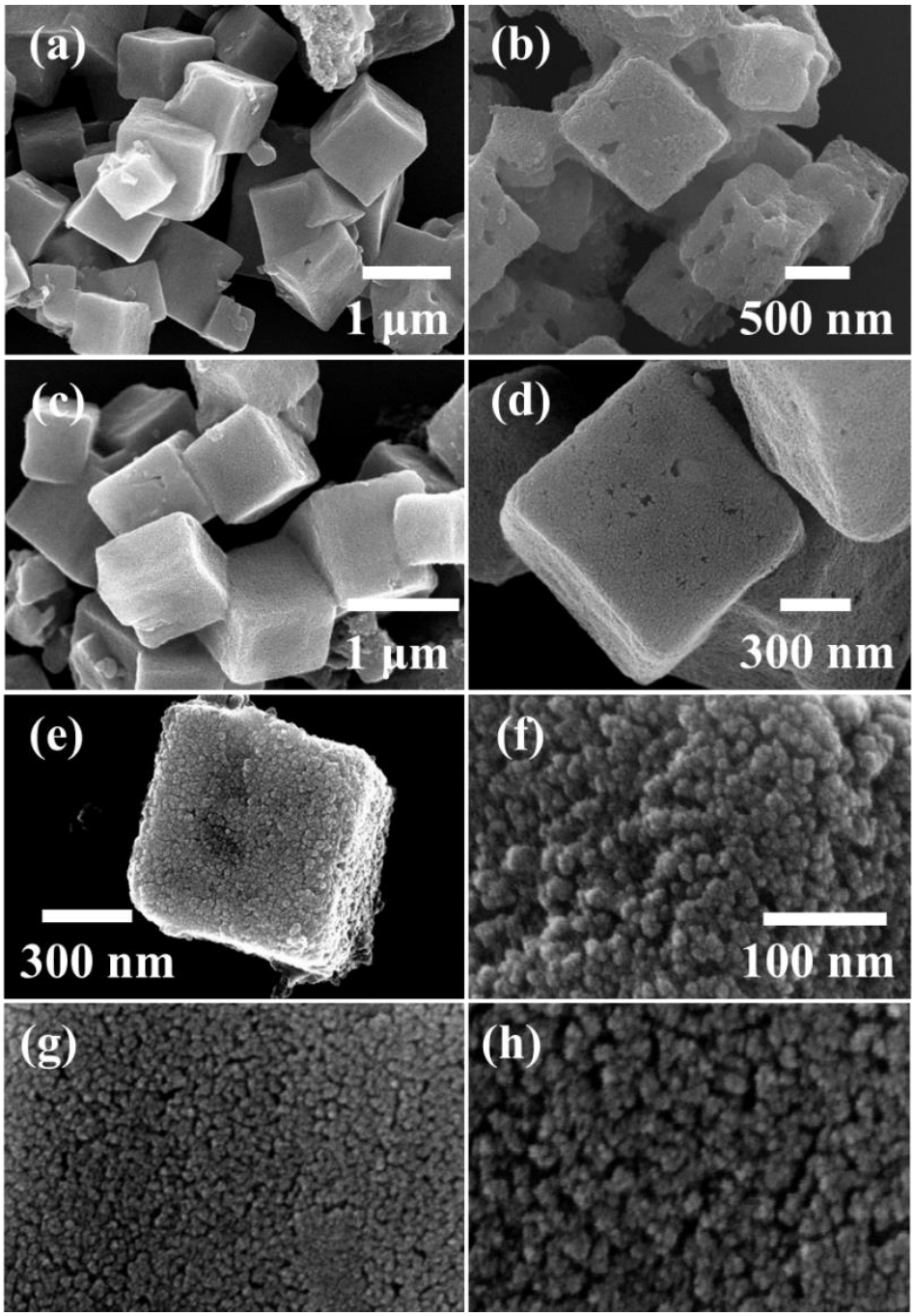

Figure S4: (a-e) SEM and (f-h) high resolution SEM images of MCFC-900.

5. TEM images of MCFC-900

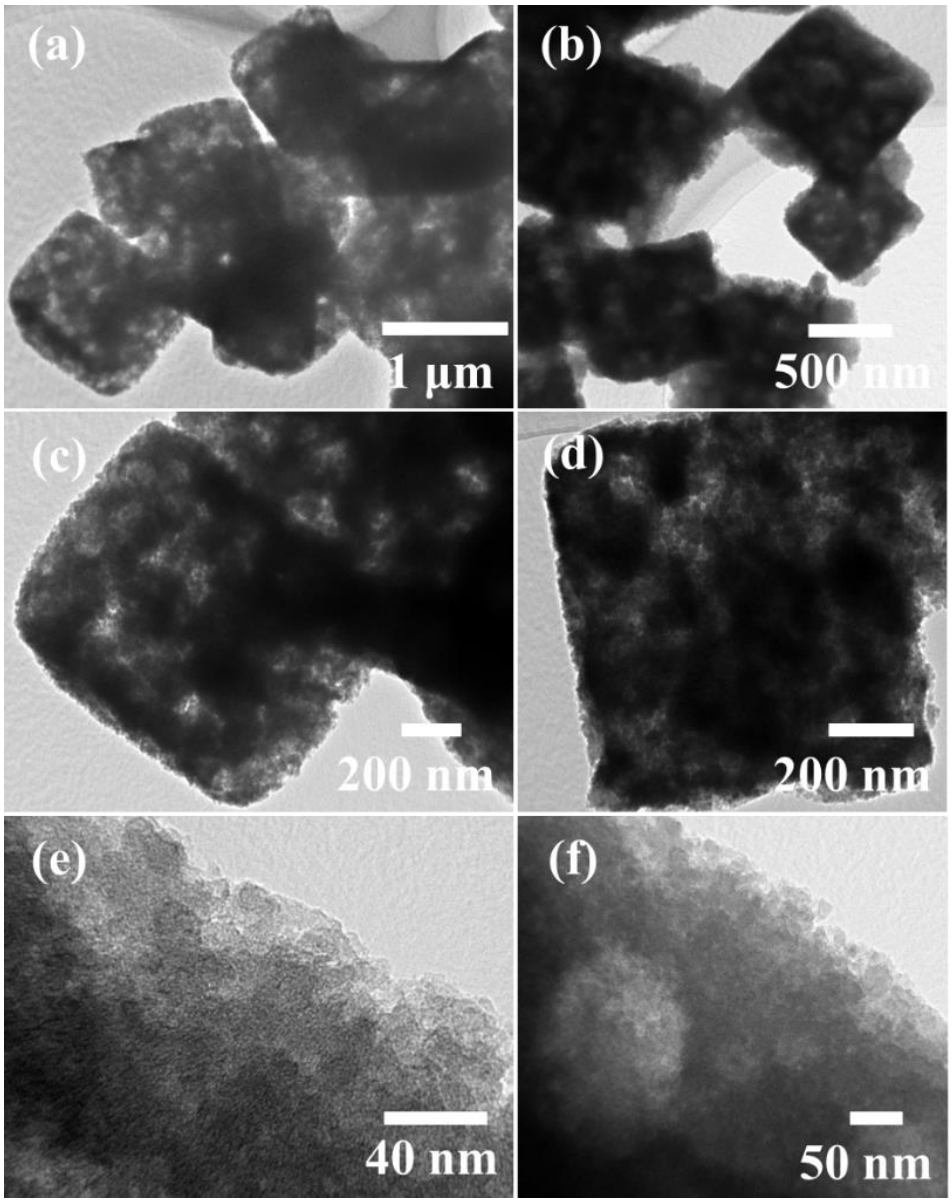

Figure S5: TEM images of MCFC-900.

6. HR-TEM images of MCFC-900

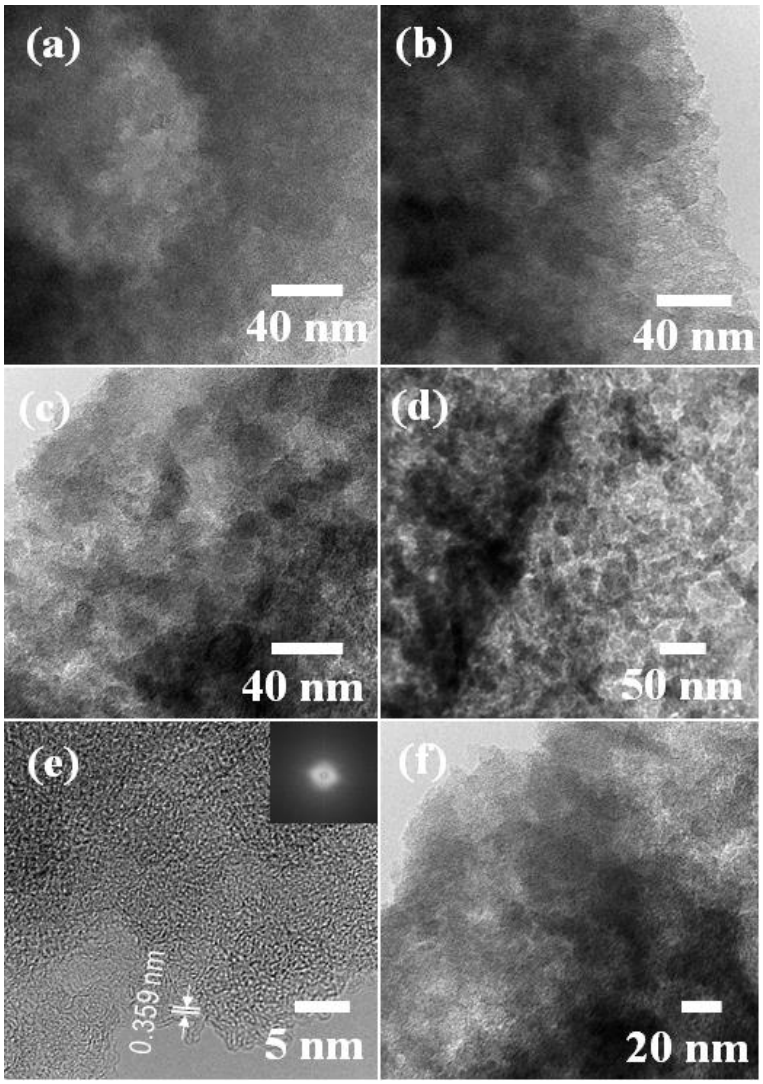

Figure S6: High resolution (HR) TEM images of MCFC-900.

7. SEM images of MCFC-2000

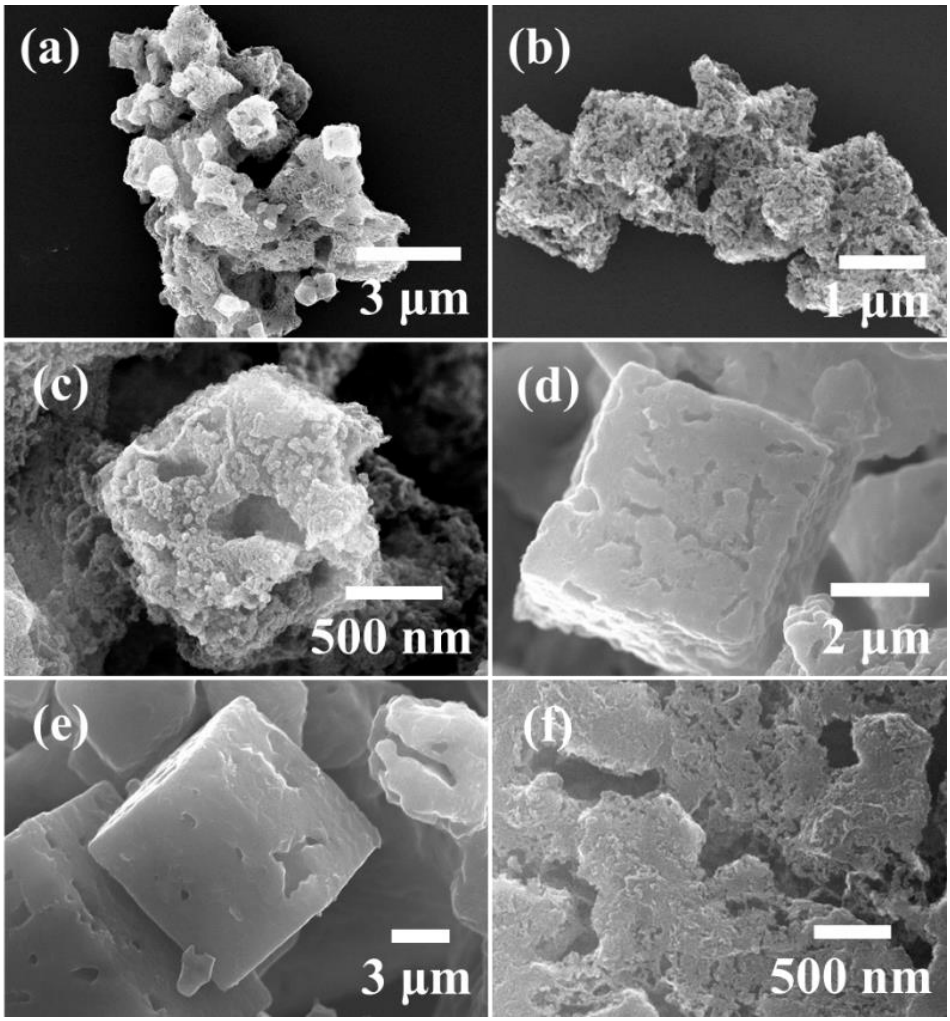

Figure S8. SEM images of MCFC-2000.

8. TEM images of MCFC-2000

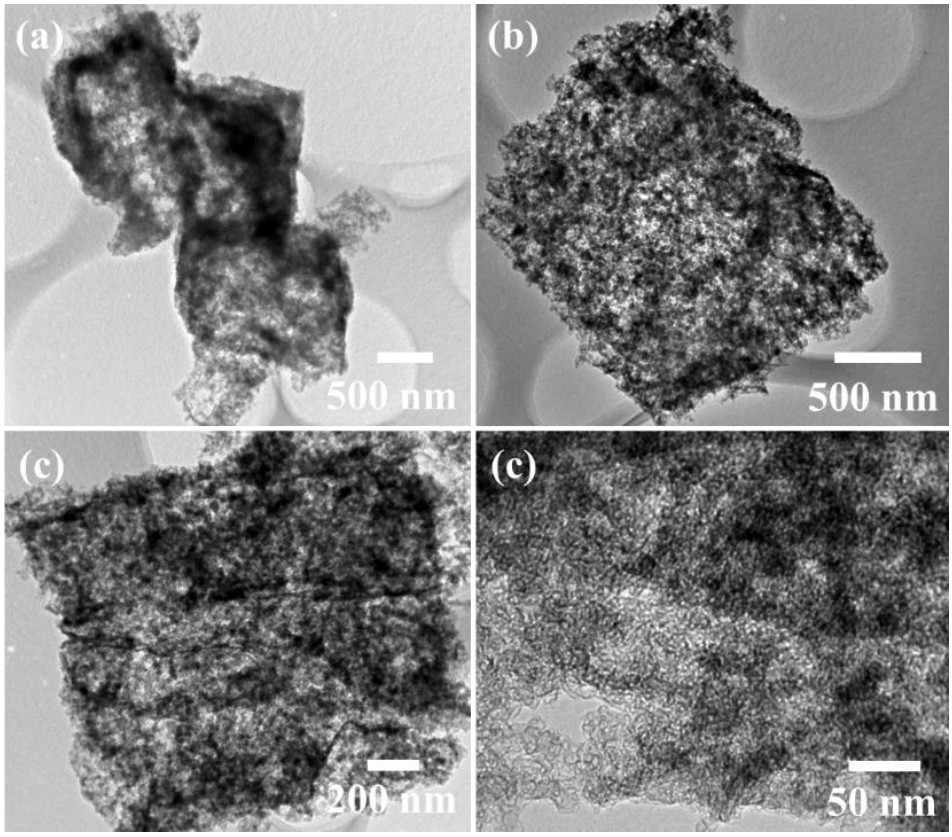

Figure S9: TEM images of MCFC-2000.

9. HR-TEM images of MCFC-2000

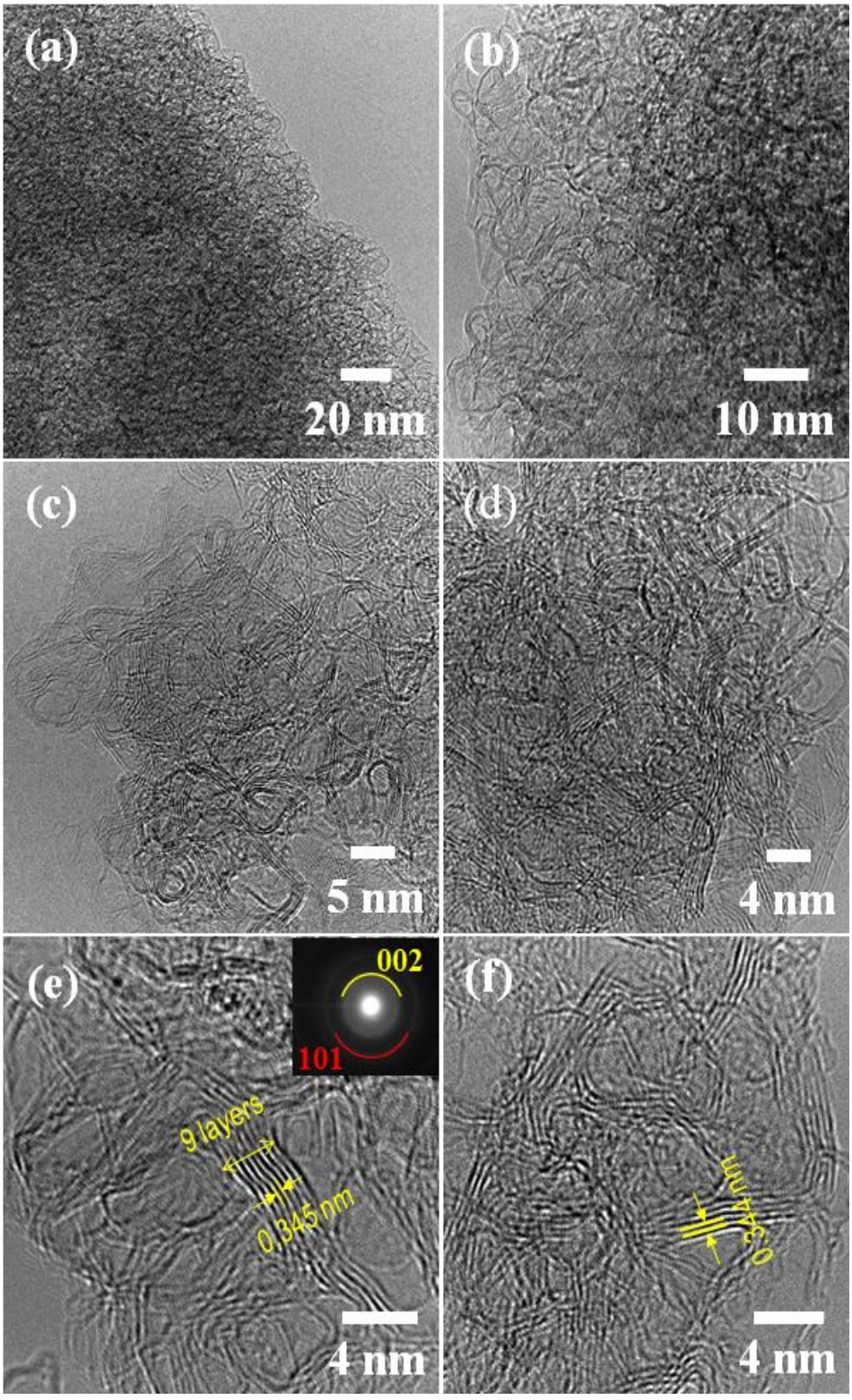

Figure S10: HR-TEM images of MCFC-2000.

10. Pore size distribution from BJHA method

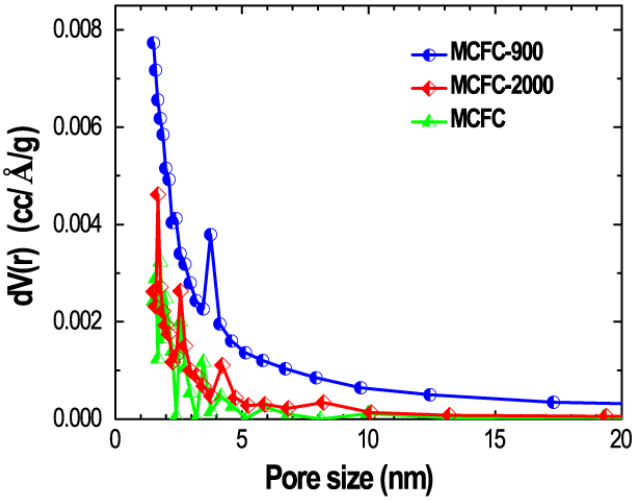

Figure S11: Pore size distributions of MCFC, MCFC-900 and MCFC-2000 obtained from BJHA method.

11. Porosity properties of MCFC, MCFC-900 and MCFC-2000.

Table S1. Porosity properties of MCFC before and after heat-treatments.

Sample	S_{BET} (m^2/g)	S_{mic} (m^2/g)	S_{meso} (m^2/g)	V_t (cc/g)	V_{mic} (cc/g)	V_{meso} (cc/g)
MCFC	47.7	19.8	27.9	0.111	0.048	0.065
MCFC_900	642.6	498.7	143.9	0.821	0.435	0.367
MCFC_2000	76.1	32.0	44.1	0.177	0.077	0.103

Table S2. Comparison of pore size obtained from BJHD and BJHA methods.

Sample	Pore size (nm) BJHD	Pore size (nm) BJHA	Pore size (nm) (Average)
MCFC	3.45	3.55	3.50
MCFC_900	3.89	3.00	3.44
MCFC_2000	3.09	3.33	3.21

Table S3. Comparison of mesopore volume obtained from BJHD and BJHA methods.

Sample	V_{meso} (cc/g) BJHD	V_{meso} (cc/g) BJHA	V_{meso} (cc/g) (Average)
MCFC	0.063	0.068	0.065
MCFC_900	0.386	0.349	0.367
MCFC_2000	0.100	0.107	0.103

Table S4. Comparison of surface area from BJHD and BJHA methods.

Sample	S_{meso} (m^2/g) BJHD	S_{meso} (m^2/g) BJHA	S_{meso} (m^2/g) Average
MCFC	25.2	30.6	27.9
MCFC_900	167.8	120.1	143.9
MCFC_2000	44.5	43.7	44.1

12. Additional XPS data

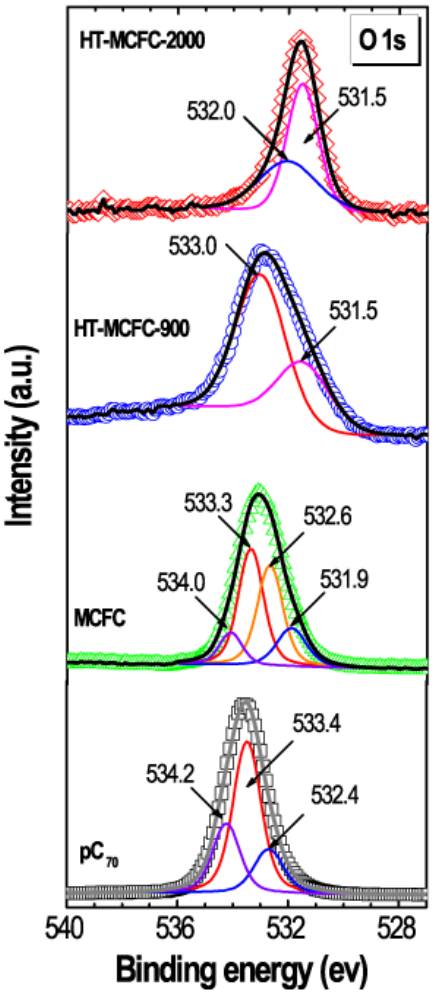

Figure S~~12~~1 O 1s core level XPS spectra with peak fit.

13. CV curves of MCFC and calculated specific capacitance

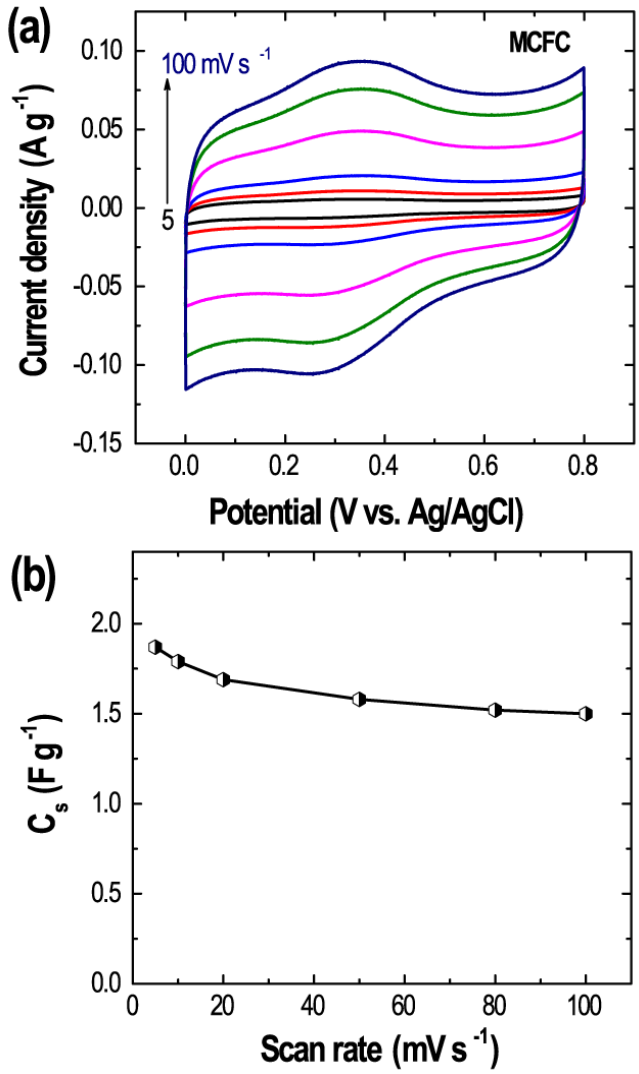

Figure S13: (a) CV curves, and (b) specific capacitance vs scan rate plot of MCFC.

14. CV curves of MCFC-1500 and MCFC-2000

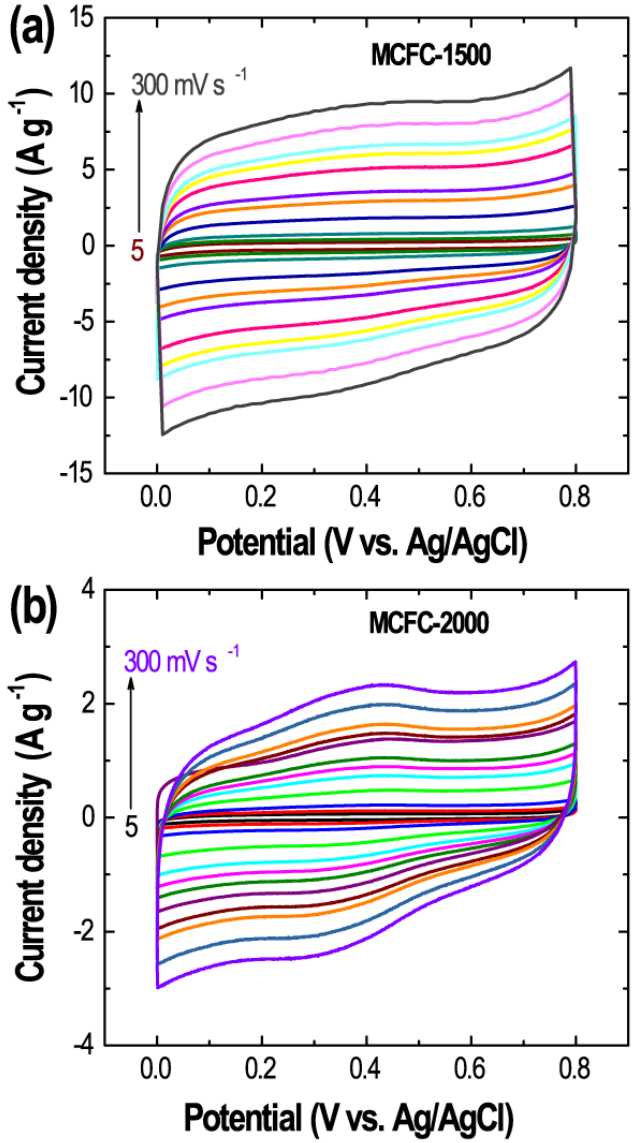

Figure S14: (a) CV curves of MCFC-1500 at different scan rates (5, 10, 20, 50, 80, 100, 200, and 300 mV s^{-1}) and (b) Corresponding CV curves for MCFC-2000.

15. Additional charging-discharging data

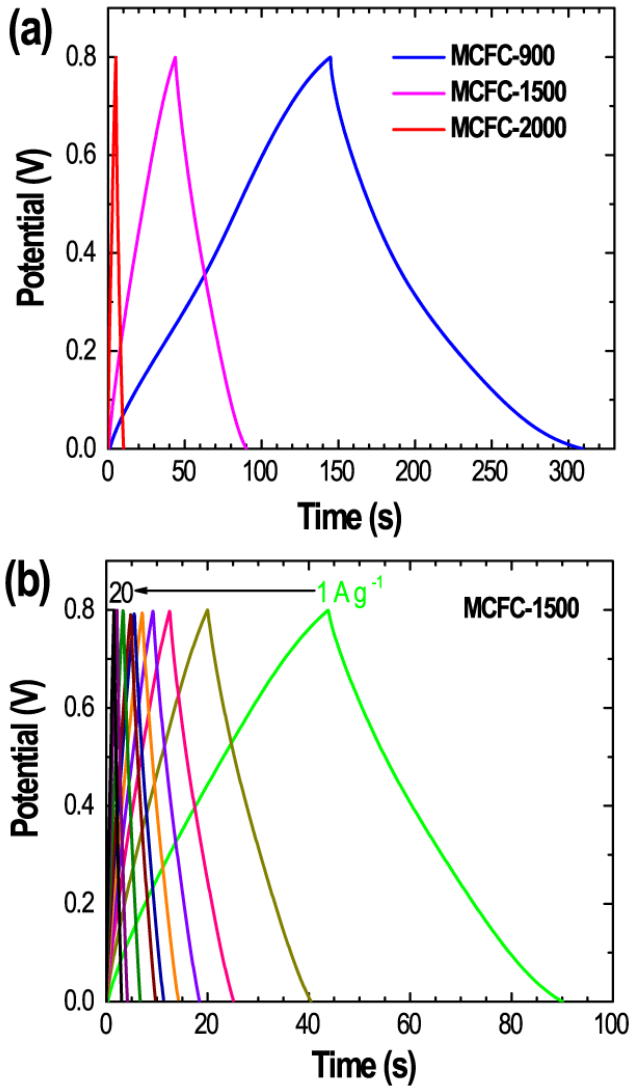

Figure S15: (a) Comparison of charge-discharge curves of MCFC-900, MCFC-1500 and MCFC-2000 at current density of 1 A g^{-1} and (b) Charge-discharge curves of MCFC-1500 at different current densities (1, 2, 3, 4, 5, 6, 7, 10, 15 and 20 A g^{-1}) as typical example.

15. Comparison of electrochemical performance of MCFC-900 with other porous carbon materials

Table S5: Comparison table of MCFC 900 with other carbon-based materials.

Materials	Specific capacitance (F g^{-1})	Scan rate or current density	Electrolyte	Ref.
Mesoporous fullerene crystals	172 141	0.5 A g^{-1} 0.5 A g^{-1}	6 M KOH Na_2SO_4	38 39
Pure graphene	101	20 mV s^{-1}	5.5 M KOH	40
Graphene aerogel	175 128	10 mV s^{-1} 50 mA g^{-1}	5 M KOH 6 M KOH	41 42
Mesoporous carbon sheets	275	1 mV s^{-1}	6 M KOH	43
Activated carbon	100 157	3 A g^{-1} 0.5 $mAcm^{-2}$	30% KOH 1.0 M Tetraethylammonium tetrafluoroborate	44 45
Conventional mesoporous carbon	205.3 41.5 259	5 mVs^{-1} 5 mVs^{-1} 1 A g^{-1}	30 wt% KOH 2M NaOH 6 M KOH	46 47 48
Nitrogen doped carbon	202 191.9	1 A g^{-1} 0.1 A g^{-1}	6 M KOH 1 M H_2SO_4	59 50
Boron doped carbon	0.26 (F m^{-2}) 228	2 mVs^{-1} 1 mVs^{-1}	6 M KOH 1 M H_2SO_4	51 52
Carbon nanotube	180 102	- 100 Hz	7.5 N KOH 38 wt % H_2SO_4	53 54
MCFC-900	**286** **205**	**5 mV s^{-1}** **1 A g^{-1}**	**1 M H_2SO_4**	**This work**